Journal of Biomedical Optics

BiomedicalOptics.SPIEDigitalLibrary.org

Lensless imaging through multiple phase patterns illumination

Anwar Hussain
Yicheng Li
Diyi Liu
Cuifang Kuang
Xu Liu

SPIE.

Anwar Hussain, Yicheng Li, Diyi Liu, Cuifang Kuang, Xu Liu, "Lensless imaging through multiple phase patterns illumination," *J. Biomed. Opt.* **22**(11), 110502 (2017), doi: 10.1117/1.JBO.22.11.110502.

Lensless imaging through multiple phase patterns illumination

Anwar Hussain,[a,b] Yicheng Li,[a] Diyi Liu,[a] Cuifang Kuang,[a,c] and Xu Liu[a,c,*]
[a]Zhejiang University, College of Optical Science and Engineering, State Key Laboratory of Modern Optical Instrumentation, Hangzhou, China
[b]COMSATS Institute of Information Technology, Department of Physics, Quantum Optics Lab, Islamabad, Pakistan
[c]Shanxi University, Collaborative Innovation Center of Extreme Optics, Taiyuan, China

Abstract. A stable optical system is required to acquire a high-quality image. A motionless lensless setup is designated to obtain high-resolution and large field of view images. The sample is sequentially illuminated with multiple random phase patterns, and the recorded images are subtracted from the system calibration images correspondingly. The resultant images are propagated to the sample plane. The summation of all images yields a final image with resolution of ~4 μm, field of view of ~15 mm^2, and better signal-to-noise ratio. This technique provides a compact, stable, and cost-effective optical system. © *2017 Society of Photo-Optical Instrumentation Engineers (SPIE)* [DOI: 10.1117/1.JBO.22.11.110502]

Keywords: image reconstruction; resolution; coherent optical system; image processing.

Paper 170545LRR received Aug. 17, 2017; accepted for publication Oct. 26, 2017; published online Nov. 11, 2017.

Lensless microscopy is mainly restricted by signal-to-noise ratio (SNR) and image reconstruction process. Such systems have a simplified geometry but a complex information retrieval process. The sample is placed very close to the sensor plane to take advantage of unit magnification as well as the compact size configuration. The phase retrieval process in conventional systems is relatively easy due to having a large configuration.[1–4] The $4f$ optical systems[5] or holographic systems[6] have been used to retrieve the recorded phase and amplitude of the sample at the sensor plane. For lensless microscopy, the diffracted higher spatial frequencies are retrieved through multiangle illumination both in the transverse[7–8] and axial directions.[9] The multiwavelength concept is also used to enhance the resolution of lensless optical systems.[10–11] The resolution of an image is also restricted by sensor pixel sampling due to large pixel size.[12–14] In lensless microscopy, this factor is corrected through $x-y$ translation of the illumination source.[8] The lensless microscopic system is made more compact through the side illumination technique[15] to reduce the complexity while achieving a large field of view. The reconstruction process is simplified through the phase mask pattern that is placed before the sample, where information of a sample is encoded.[16] This idea is carried out to improve the quality of the image without elongating the geometry of the system.

We report a stable optical system for lensless microscopy without mechanical motion of any optical component. The system consists of a laser source, a phase mask, the sample, and a CMOS sensor in a vertical column. The sample is illuminated through random phase mask patterns that are generated by a spatial light modulator (SLM) in a sequential manner. The phase value range for all phase mask patterns is fixed (0 to 2π), while distribution of the phase for each phase mask is varied. These multiple phase patterns encode the amplitude and phase of the sample, which are propagated toward the sensor. The interference pattern recorded at the sensor plane contains a real image embedded in the twin image and a self-interference term. The system is initially calibrated with different phase mask patterns, and images are recorded correspondingly. The two types of images are independently captured and mutually subtracted to obtain a set of resultant images. The resultant images are sequentially propagated to the sample plane. The summative result of these images is a final image with an improved resolution and high SNR.

The working principles of our technique are very simple and straightforward. The sample is placed in close vicinity of the imaging sensor and is illuminated with a phase pattern generated by a transmission mode SLM as shown in Fig. 1. The sample elements phase is added to the random phase of the phase mask and the phase from coherent illumination, and images are recorded at the sensor with an accumulative phase. This process gives different combinations of the elements phase at the sensor plane. The sensor is from Sony Company with a pixel size of 1.4 μm, with some restrictive electronics parts. Two main parameters that affect the image quality in our technique are sample-to-sensor distance and number of phase patterns. The measurement of hundreds of micron-level separation between sample and sensor is also critical, and the exact value for this parameter is found through a computational autofocusing method. This method is based on the sharpness of the sample elements edges. The second parameter that affects the quality of image is the number of illumination phase patterns per experiment. To find the exact value is difficult, while the probabilistic value is used as a standard value. In our case, we test the technique for 20 different phase mask patterns in both simulation and experiment. The phase retrieval relation of our proposed technique is given in Eq. (1), in which the left side shows the amplitude and phase of the sample

$$\text{amp}.\exp[i.S(\eta',\xi')] = \sum_{i=1}^{20} \frac{P_{\text{ro}}\{(I_i - I_{ri}).\exp[i.\phi_{ri}(\eta,\xi)]\}}{\text{Field}_{\text{samp}.i}(\eta',\xi')} + \text{noise}, \quad (1)$$

where the coordinates (η',ξ') and (η,ξ) represent the sample and sensor planes, respectively, while i is the running integer for summation that gives the number of experiments with different phase mask distributions. The term in bracket on the right side of Eq. (1) shows the difference of two types of images: with sample and without sample, multiplied with the numerically reconstructed phase pattern of the phase mask at the sensor plane correspondingly. The term P_{ro} gives the propagation function, which propagates the square bracket term to the sample

*Address all correspondence to: Xu Liu, E-mail: liuxu@zju.edu.cn

1083-3668/2017/$25.00 © 2017 SPIE

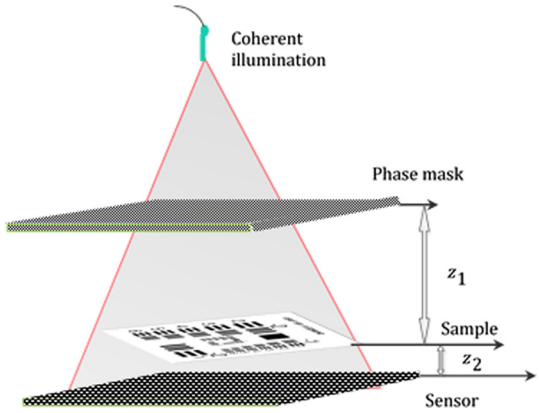

Fig. 1 Wide-field lensless microscopy using multiple phase masks illumination: z_1 (phase mask-to-sample distance) and z_2 (sample-to-sensor distance).

plane. The numerically retrieved phase pattern of the phase mask is propagated to the sample plane from the sensor plane using an angular spectrum propagation method. In Eq. (1), the denominator term represents the phase pattern during each illumination. The noise term shows the background noise and evenly distributed twin image effect throughout the retrieved sample image. This relation replaces the iterative process of phase and amplitude retrieval in lensless microscopy. In Eq. (1), the key factor is the phase mask pattern ϕ_r, whose distribution was changed before every illumination. The sequential illumination encodes the phase and amplitude information of the sample, and the image is recorded at the sensor plane, respectively. The alteration of the phase distribution at the individual phase mask will update the final image phase at the sensor plane. This process will help to improve the SNR of the reconstructed image at the sample plane. The 20 different phase masks illumination process is like the iteration process that updates phase and amplitude at the sensor plane.

The technique is verified through simulation and experiment. In simulation, the USAF 1951 resolution target is used as a sample having vertical and horizontal groups of lines. The field of view for our simulation is 15 mm^2, which is equal to the active area of the image sensor in lensless microscopy. The simulation results are presented for comparison, as shown in Fig. 2. The sample captured without using the phase mask is compared with images recovered using single-phase pattern illumination and multiple phase patterns illumination in Figs. 2(a)–2(c). With the proposed technique, the twin image artifacts in (a) are suppressed, and the low SNR in (b) is improved. Thus, the image resolution of the multiple phase patterns illumination technique is much better than the other two methods. In addition, the image retrieved with this technique has approximately the same level of resolution as the image obtained through multiangle illumination for which the phase pattern is fixed, as shown in Fig. 2(d).[17] The main difference is the imaging process as well as the system compactness. The multiangle illumination method has a more complex imaging processing procedure and a less compact system when compared with this technique, but they share the same resolution.

A more authentic verification of our technique is carried out in the laboratory. For this technique, the laser with a wavelength of 641 nm is from Coherent Company, and the SLM working in transmission mode is from Daheng Company. The USAF 1951 resolution chart is from Edmund Optics with maximum resolution of about 1 μm but ~4 μm for group 7. The phase mask plane is fixed at 9.6 cm above the sample while a sensor is placed beneath the sample with the distance of about 750 μm correspondingly. The experimental results are shown in Fig. 3, in which (a) is the raw image obtained directly from the sensor for single-phase pattern illumination, (b) is the final image because of multiple phase patterns illumination, and (c) is the final image as a result of multiangles phase masks illumination.[17] In each row of Fig. 3, the first image gives the entire field of view image and the second one is the central magnified portion of the corresponding image. The visual comparison of all the three images validates our technique. For a more detail analysis, the central part of all the images, groups 6 and 7, is magnified. The improved resolution is quantified through the magnified portion, which is approximately equal for Figs. 3(b) and 3(c). However, the innovative point is the stable and compact system for our recent technique. The comparison of our recent technique in Fig. 3(b) with the other images in Fig. 3 clearly validates the improvement of the system based on optical geometry and the imaging process. The mutual comparison of these magnified images further endorses our technique. In Figs. 4(a) and 4(b), the phase information of our sample obtained from the multiple phase patterns illumination technique is compared with that of the single-phase mask image profile. The sharp edges of Fig. 4(b) reveal the high phase image quality with a significant value of SNR. The quantitative analysis of the SNR versus the number of illumination patterns is presented in Fig. 5. This graph beautifully explains the trend of SNR with the increment of the number of illumination patterns. The graph shows the increasing trend of SNR as the number of illuminations increased. The graph becomes saturated at the higher values, which means that a further increase in number of illuminations will collect noise instead of useful information. This collection of noise will increase the computational time rather than enhance the resolution.

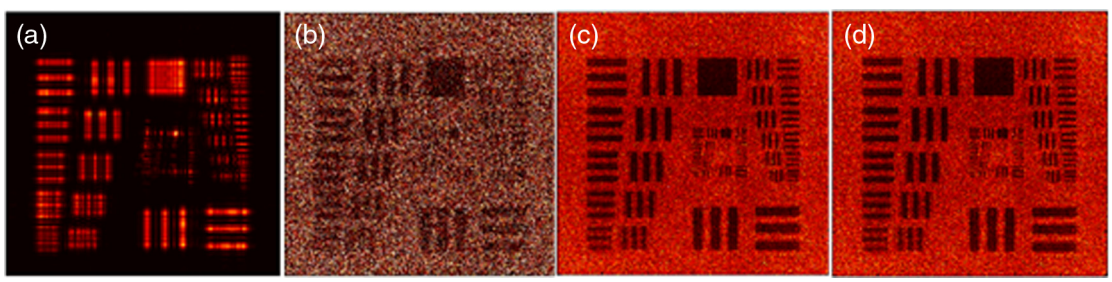

Fig. 2 Simulation results: (a) image retrieved without phase mask, (b) the resultant image of single-phase mask illumination, (c) resultant image after 20 phase patterns sequential illumination, and (d) resultant of multiangles of illumination.

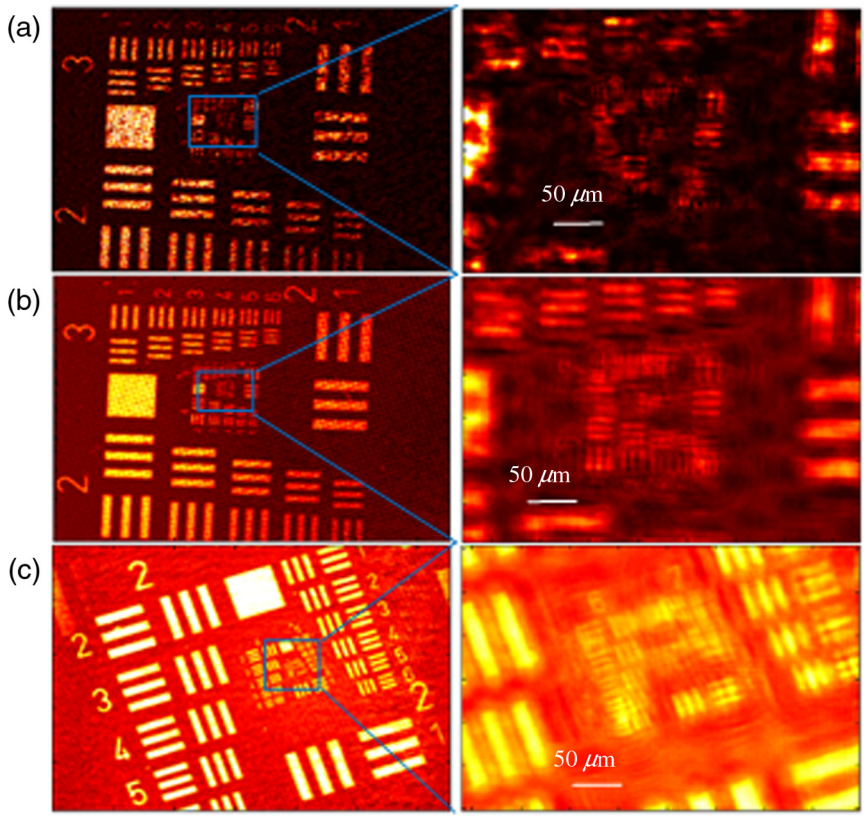

Fig. 3 Experimental results: (a) the images obtained with single phase mask, (b) the final image obtained as the result of multiple phase masks illumination, and (c) the images retrieved using multiangles of illumination.

The phase information of the phase mask strengthens the idea of retrieving the sample information along the axial direction for three-dimensional samples for future work.

In conclusion, the innovation of this technique is the stable optical setup without any translation or rotational motion. This is the turning point in lensless microscopy, in which the resolution and SNR are simultaneously improved with a compact size system.

Such systems are highly demanded for optical imaging in remote areas, which are out of reach for large optical systems. Our reported compact system can be placed anywhere due to its portable attribute. To commercialize the system, several modifications have been suggested: manufacturing of a sensor with a protuberant active area and compact illumination assembly. However, there is a trade-off between the number of phase patterns illumination and the imaging speed. For future work, the simultaneous illumination of random phase patterns to retrieve the sample information in a single step is recommended. This will improve the speed of the imaging process. This type of optical system is designated to provide a compact and cost-effective microscope. The best option in this regard is the transmission-mode imaging, in which the sample is placed near the image sensor at a distance of a few microns. To translate the setup into reflection mode, the geometrical shape will be changed into a little bulky system to capture the images. The working principles for such a type of system remain the same with modified geometry from compact to a little bulky. The goal of such a type of system is to take an image of biological tissue to diagnose an infection with high resolution and precision at a minor level. The system will work for biological tissues both in shadow imaging and fluorescence imaging schemes. In Fig. 4, our phase retrieval claim is strengthened for the

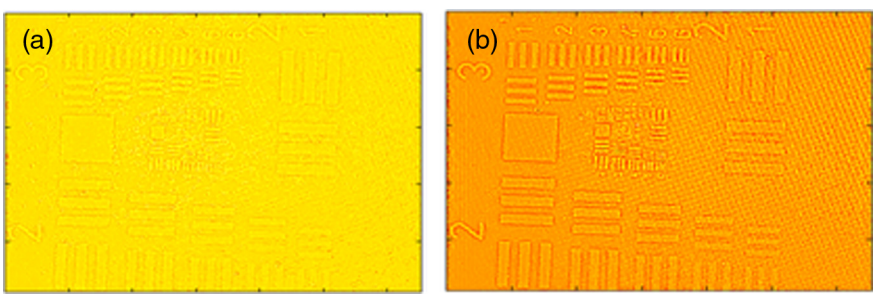

Fig. 4 Simulation results: (a) the phase profile of resultant image of single-phase mask illumination and (b) the phase profile of the resultant image after 20 phase patterns sequential illumination.

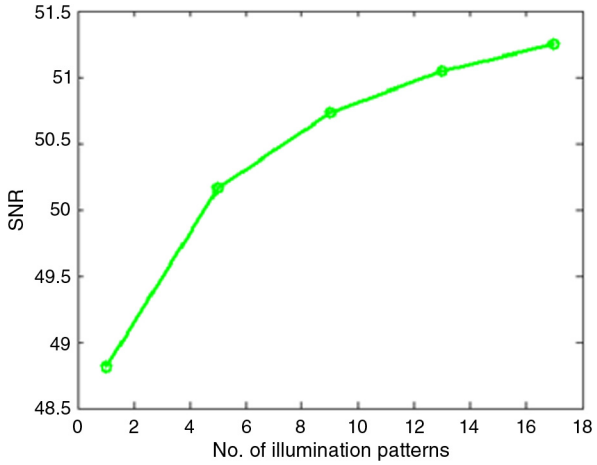

Fig. 5 Graph of SNR versus number of illumination patterns.

USAF 1951 resolution chart. In the case of biological tissues, the imaging technique of multiple phase patterns illumination will remain the same with sample replacement.

Disclosures

The authors declare no competing financial interests.

Acknowledgments

This work was supported by the National Basic Research Program of China (973 Program) (No. 2015CB352003), the National Key Research and Development Program of China (No. 2016YFF0101400), the National Natural Science Foundation of China (Nos. 61335003, 61377013, 61378051, and 61427818), the Natural Science Foundation of Zhejiang Province (No. LR16F050001), and the Fundamental Research Funds for the Central Universities (No. 2017FZA5004).

References

1. A. Grjasnow et al., "Phase resolving microscopy by multi-plane diffraction detection," *J. Microsc.* **231**(1), 115–123 (2008).
2. D. J. Lee and A. M. Weiner, "Optical phase imaging using a synthetic aperture phase retrieval technique," *Opt. Exp.* **22**(8), 9380–9394 (2014).
3. Q. Lin et al., "Super-resolution imaging in digital holography by using dynamic grating with a spatial light modulator," *Opt. Lasers Eng.* **66**, 279–284 (2015).
4. Y. Zhang et al., "Phase retrieval microscopy for quantitative phase-contrast imaging," *Optik—Int. J. Light Electron Opt.* **115**(2), 94–96 (2004).
5. A. Hussain and J. L. Martínez Fuentes, "Resolution enhancement using simultaneous couple illumination," *J. Opt.* **18**(10), 105702 (2016).
6. C. Quan et al., "Temporal phase retrieval from a complex field in digital holographic interferometry," *Opt. Lett.* **32**(12), 1602–1604 (2007).
7. T. W. Su et al., "Multi-angle lensless digital holography for depth resolved imaging on a chip," *Opt. Exp.* **18**(9), 9690–9711 (2010).
8. W. Luo et al., "Synthetic aperture based on-chip microscopy," *Light: Sci. Appl.* **4**, e261 (2015).
9. C. Zuo et al., "Lensless phase microscopy and diffraction tomography with multi-angle and multi-wavelength illuminations using a LED matrix," *Opt. Exp.* **23**(10), 14314–14328 (2015).
10. P. Bao et al., "Lensless phase microscopy using phase retrieval with multiple illumination wavelengths," *App. Opt.* **51**(22), 5486–5494 (2012).
11. W. Luo et al., "Pixel super-resolution using wavelength scanning," *Light: Sci. Appl.* **5**, e16060 (2016).
12. A. Greenbaum et al., "Increased space-bandwidth product in pixel super-resolved lensfree on-chip microscopy," *Sci. Rep.* **3**, 1717 (2013).
13. W. Bishara et al., "Holographic pixel super-resolution in portable lensless on-chip microscopy using a fiber-optic array," *Lab Chip* **11**(7), 1276–1279 (2011).
14. D. Ryu et al., "Subsampled phase retrieval for temporal resolution enhancement in lensless on-chip holographic video," *Biomed. Opt. Exp.* **8**(3), 1981–1995 (2017).
15. M. Rostykus et al., "Compact lensless phase imager," *Opt. Exp.* **25**(4), 4438–4445 (2017).
16. S. Bernet et al., "Lensless digital holography with diffuse illumination through a pseudo-random phase mask," *Opt. Exp.* **19**(25), 25113–25124 (2011).
17. A. Hussain et al., "On-chip microscopy using random phase mask scheme," *Sci. Rep.* **7**, 14768 (2017).